Design Criteria and Measurements of the Prototype of the DAΦNE Accumulator Cavity

S. Bartalucci, R. Boni, A. Gallo, H. Hsieh, G. Raffone and B. Spataro
I.N.F.N., Laboratori Nazionali di Frascati
C. P. 13, 00044 Frascati, Rome (Italy)

Abstract

This paper deals with the design criteria of the accumulator RF cavity of the Frascati 510 MeV Φ-Factory DAΦNE. Particular care was given in defining the cavity geometry in order not to have resonant electron loading. Other important engineering aspects, such as cooling and thermal effects, are outlined. The possibility of damping the parasitic cavity modes is investigated and the preliminary RF tests on a copper prototype are presented.

1. INTRODUCTION

The Φ-Factory project at LNF [1] includes an accumulator ring to store electrons or positrons injected from the 510 MeV Linac before filling the main rings. A single 130 mA bunch will be stored in the accumulator and extracted at a 1 Hz rate for the injection in the DAΦNE rings.

The main parameters of the Accumulator Radiofrequency (RF) System are listed in Table 1. The RF frequency is exactly one fifth of the main ring to synchronize the injection into any desired bucket of DAΦNE [2]. An accelerating cavity peak voltage of 200 kV is also required to have large energy acceptance. The beam synchrotron and parasitic losses are estimated to be about 3.6 kW.

Table 1
Accumulator RF System main parameters

RF Frequency	73.651 MHz
Harmonic number	8
RF Peak Voltage	200 kV
RF Energy Acceptance	2.38 %

2. CAVITY DESIGN CRITERIA

Due to the low operating frequency and the short straight section available in the accumulator (1.2 m), the cavity is necessarily a reentrant single ended coaxial resonator which is compact in size and simple to manufacture. The cavity drawing is shown in Fig.1. The profile of the surface has been studied in order not to have multipacting (mp) that often makes the cavity operation unreliable. The computer code Newtraj [3] has been run to predict the areas of the inner cavity surface where the resonant electron loading is most probable. The cavity profile was then optimized according to the results given by the code.

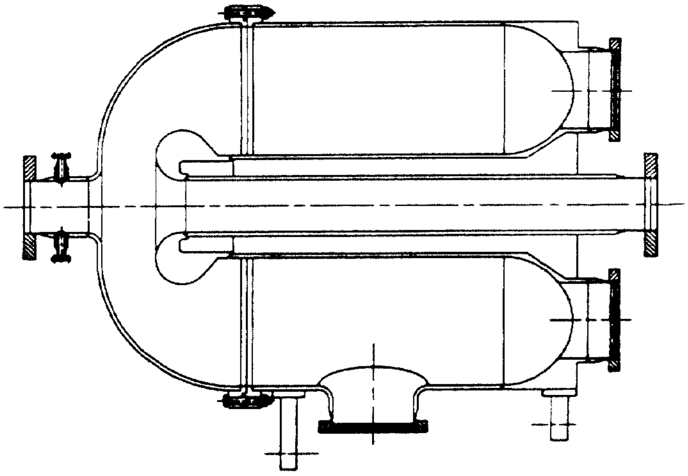

Figure 1. Profile of the Accumulator Cavity

In Fig. 2 is shown the only mp trajectory evidenced by Newtraj. In some cases, RF conditioning is helpful to cure mp but a moderate coating of TiN on those areas should however be necessary.

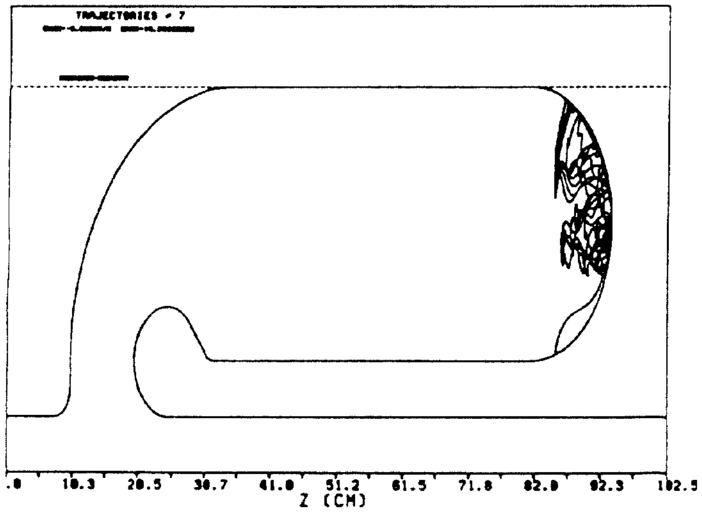

Figure 2. Simulation of a mp trajectory at 190 kVp.
(Cavity not to scale)

The cavity will be fabricated with OFHC copper to ease the cooling and reduce the dissipated RF power. Also, the use of copper is well suited for ultra high vacuum.

The cavity will be coupled with a loop to the 6-1/8" RF coaxial line and tuned with a cylindrical plunger both located in the magnetic field region of the accelerating mode. An additional port on the cavity body is foreseen to connect a vacuum pump.

3. PROTOTYPE TESTING

A copper sheet full scale prototype, shown in Fig.3, was tested in laboratory. The capability of a 116 mm diameter plunger of tuning the cavity over a temperature range 20+40°C has been checked; the maximum tuner penetration is 3 cm.

The needed coupling factor with the RF station is $\beta = 1.26$ and has been set by rotating the RF input loop.

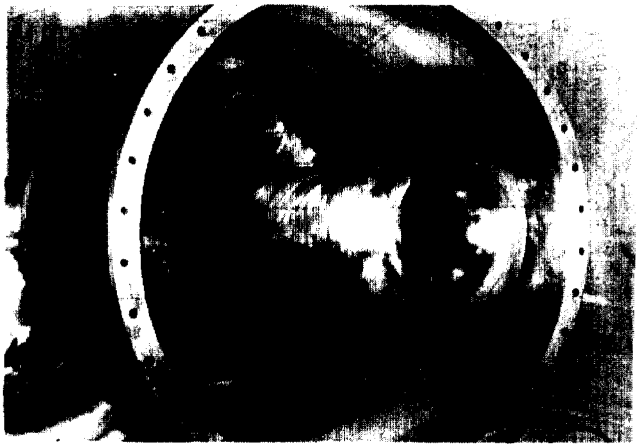

Figure 3. The cavity prototype before testing.

Table 2
Accumultor cavity parameters

	(calculated)	(prototype)
RF Frequency	73.651 MHz	(73.607)
Unloaded Qo	22,000	(19,000)
Shunt Impedance ($V^2/2P$)	1.74 MΩ	(1.50)
Peak Gap Voltage	200 kV	
Cavity wall losses	13.3 kW	
Beam power	3.5 kW	
Coupling factor β	1.26	
Max Surface Electric Field	3.9 MV/m	
Max Axial Electric Field	1.48 MV/m	
Cavity length	900 mm	
Cavity diameter	750 mm	
Gap length	100 mm	

The cavity spectrum has been measured with the network analyzer HP8753C and compared with that calculated with URMEL code. Table 3 reports a list of high order modes (HOM) monopoles and dipoles till 1 GHz which lay very close to a beam spectrum line (that are 9 MHz spaced). In fourth column we list the Q values of these HOM obtained connecting three damping loops to the cavity (two loops are at 90° with respect to each other for coupling the two polarizations of the dipole modes). The (R/Q)'s were measured with the perturbation method [4]. Since the particular cavity shape, the modes may not be classified as usual in technical literature.

Table 3

Monopoles	*Freq.(MHz]*	*Qo*	Q_L	*R/Q (Ω)*
TM0-5	607.94	11000	50	0.6
TM0-8	783.36	7000	1500	0.82
TM0-9	884.51	5500	750	0.70
Dipoles	*Freq.(MHz]*	*Qo*	Q_L	*R/Q (Ω)*
1MM-6	709.43	7000	1000	0.31
1MM-7	722.66	3000	500	0.17
1MM-9a	801.15	17400	5300	1.86
1MM-9b	801.64	18000	4200	1.86
1MM-10	828.78	6300	70	0.2

4. COOLING CRITERIA

The heat load due to the RF wall losses (about 13.3 KW) can be removed by means of copper cooling pipes simply brazed on the external surface of the cavity; then the wall temperatures are kept constant as the influence of the surrounding environment (i.e. air temperature) is practically negligible.

A temperature field evaluation can be carried out by means of a finite element analysis [5] and it may be useful to check, during the mechanical design, the behaviour of the cooling system; in other words the design parameters (as pipes number, position and diameter, mass flow rates) can be varied to achieve an optimal arrangement between the cavity permissible deformations and the cooling system requirements; this kind of approach can be useful also from a cost reduction point of view.

In this thermal analysis the quality of brazings plays an important role from the heat exchange point of view; as the effective contact area depends on both the brazing process and the geometry of the surfaces, care must be given during the computation of the real heat exchange coefficient; theoretically the worse obtainable coefficient depends roughly on the ratio between the water convective coefficient and the pipe thermal conductivity, the pipe equivalent diameter and the thickness of the pipe.

Fig. 4 shows the temperature solution of one of the configurations taken into account.

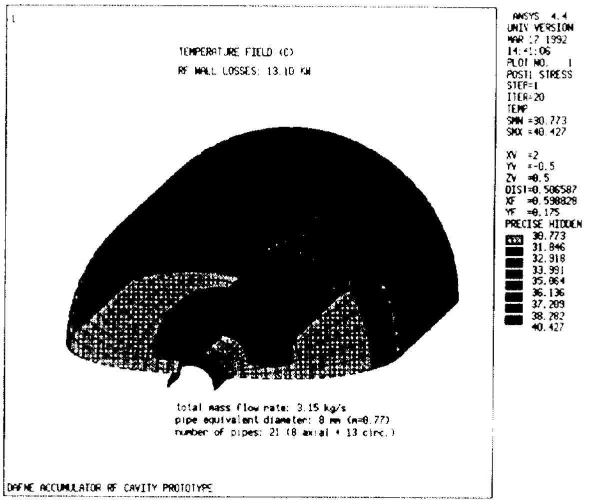

Figure 4. Cavity temperature field.

A structural analysis has also been perfomed in order to evaluate the deformations induced by the temperature gradients (see fig. 5); the total variation of the cavity resonant frequency can also be easily computed by means of the displacements solution and the Slater Theorem.

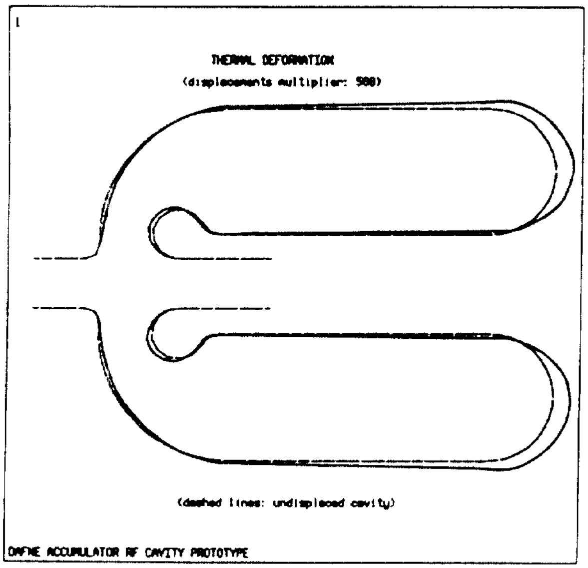

Figure 5. Thermal deformation (greatly amplified).

The dependence of the cavity volume due to the inlet water temperature changes and the mass flow rate changes is shown in fig. 6, where the variations of the cavity resonant frequency are plotted versus the difference between the inlet water temperature Tiw and an "operating temperature" To.

Of course these results depend on the structural boundary conditions of the cavity; in this case the cavity gap does not expand freely and the resonant frequency depends on the volume variations of the regions of only magnetic field as fig. 5 shows. Further computations are still in progress.

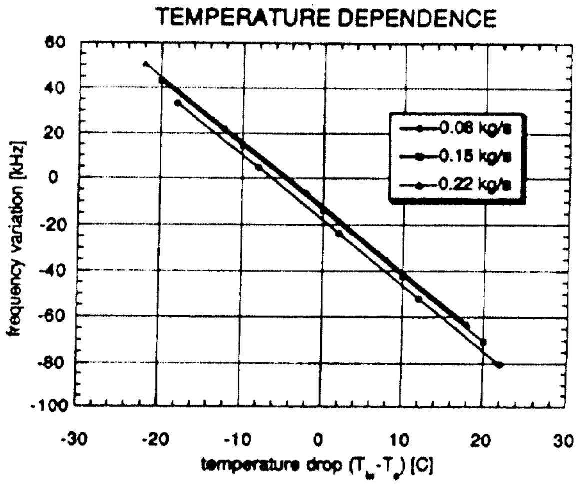

Figure 6. Temperature dependence of the cavity frequency.

5. ACKNOWLEDGEMENTS

The RF tests would have not been possible without the support of the RF technicians P. Baldini, F. Lucibello and S. Quaglia. Also special thanks are due to G. Fontana for the mechanical design of the cavity.

6. REFERENCES

[1] The DAΦNE Project Team, "DAΦNE Status Report", this conference.

[2] R.Boni, S.Kulinski, M.Preger, B.Spataro, M.Vescovi, and G.Vignola, " The Frascati Φ-Factory Injection System", Proc. of the Particle Accelerator Conference, S. Francisco, May 1991 (to be published).

[3] R.Boni, V.Chimenti, P.Fernandes, R.Parodi, B.Spataro and F.Tazzioli, " Design and Operation of a Multipacting Free 51.4 MHz RF Accelerating Cavity ", Nuclear Instruments and Methods in Physic Research, A274, pp. 49-55, 1989.

[4] L.C.Maier and J.C.Slater, " Field Strength Measurements in Resonant Cavities ", Journal of Applied Physics, Vol.23, n. 1, January 1952.

[5] ANSYS, Swanson Analysis System Inc., Houston, Pennsylvania, 15342 (USA).